Calcium Carbonate Modifications in the Mineralized Shell of the Freshwater Snail *Biomphalaria glabrata*

Bernd Hasse,[a] Helmut Ehrenberg,[b, c] Julia C. Marxen,[d] Wilhelm Becker,[d] and Matthias Epple*[a]

Abstract: The mineralized shell (consisting of calcium carbonate) of the tropical freshwater snail *Biomphalaria glabrata* was investigated with high resolution synchrotron X-ray powder diffractometry and X-ray absorption spectroscopy (EXAFS). Parts from different locations of the snail shell were taken from animals of different age grown under various keeping conditions. Additionally, eggs with ages of 60, 72, 120, and 140 hours were examined. Traces of aragonite were found as first crystalline phase in 120 h old eggs, however, Ca K-edge EXAFS indicated the presence of aragonitic structures already in the X-ray amorphous sample of 72 h age. The main component of the shell of adult animals was aragonite in all cases, but in some cases minor amounts of vaterite (below 1.5%) are formed. The content of vaterite is generally low in the oldest part of the shell (the center) and increases towards the mineralizing zone (the shell margin). In juvenile snails, almost no vaterite was detectable in any part of the shell.

Keywords: bioinorganic Chemistry · biomineralization · crystal growth · EXAFS Spectroscopy · solid-state chemistry

Introduction

The utilization of solid inorganic materials (minerals) is widespread in the living nature. Prominent examples are skeleton structures (e.g., bone, mollusk shells, radiolaria) and functional tools (e.g,. teeth, sea-urchin spines, gravity sensors). About 60 minerals are used for such purposes by lower and higher organisms,[1] with the most widespread being calcium carbonate (especially in marine organisms), calcium phosphate (mineralized part of the skeleton of vertebrates), and amorphous silicon dioxide (found in many plants). The biologically-controlled process leading to such minerals is commonly termed as "biomineralization" (see, e.g., refs. [1–6] for recent reviews).

The main mechanisms have been identified as crystal nucleation, crystal growth and crystallization in spatially confined compartments, all of them being thoroughly regulated by the organism. Highly optimized biomacromolecules (proteins, carbohydrates, glycoproteins, proteoglycans) were developed during the evolution to control these (physicochemical) processes, for example by preferential adsorption on distinct crystal faces that leads to nucleation of defined solid phases and to morphological control of the growing crystal. Their synthesis is under strict metabolic control of the mineralizing organism.

However, there remains a large gap between the understanding of chemical model systems[7–13] and the biochemical/physiological processes that control protein and matrix formation.[14–17] In order to contribute to closing this gap, we have studied the inorganic part of the calcium carbonate shell of the fresh-water snail *Biomphalaria glabrata* with high-end solid state chemical methods. As many results on the biological mechanisms of biomineralization have been obtained earlier on this organism,[14, 16, 18–20] it can be considered as model to study the mineralization process employing an interdisciplinary approach.

Different locations of the shells of animals of various ages and different keeping conditions were studied with high-resolution diffraction in order to investigate its crystallographic phase composition. Furthermore, the initial process of shell formation in eggs was studied by X-ray diffraction and by X-ray absorption spectroscopy. The latter technique is sensitive to non-crystalline phases (e.g., amorphous solids) as well. Its main power lies in the determination of accurate

[a] Prof. Dr. M. Epple, Dipl.-Chem. B. Hasse
Solid State Chemistry
Faculty of Chemistry, University of Bochum
44780 Bochum (Germany)
Fax: (+49) 234-3214-558
E-mail: matthias.epple@ruhr-uni-bochum.de

[b] Dr. H. Ehrenberg
Hamburger Synchrotronstrahlungslabor (HASYLAB)
Deutsches Elektronen-Synchrotron (DESY)
Notkestrasse 85, 22603 Hamburg (Germany)

[c] Dr. H. Ehrenberg
Darmstadt University of Technology, Materials Science
Petersenstrasse 23, 64287 Darmstadt (Germany)

[d] Dr. J. C. Marxen, Prof. Dr. W. Becker
Department of Zoology, University of Hamburg
Martin-Luther-King-Platz 3, 20146 Hamburg (Germany)

  0947-6539/00/0620-3679 $ 17.50+.50/0

bond distances around the excited element (in this case: calcium).

Results and Discussion

The shell of adult tropical freshwater snails *Biomphalaria glabrata* consists of aragonite whose growth and morphology is controlled by small amounts of an organic matrix (ca. 0.9 wt %) consisting of polymeric protein/carbohydrate structures.[14, 16] The formation of the shell in *Biomphalaria glabrata* starts during embryogenesis in eggs.

The embryos of *Biomphalaria glabrata* develop very quickly: If kept at 25 °C they leave their egg capsules fully developed after about six days. The shell building starts early during embryogenesis.[21] The developmental stages at 25 °C are as follows: After 40 – 45 h of development the prospective shell field can be observed. In the center of the shell field a narrow channel invaginates like the finger of a glove ("shell field invagination", SFI). After 48 h the invagination closes apically, and after 50 h the first single-layered periostracum (an outer protective shield of the shell consisting of polymeric organic material) appears on the shell field. A Veliger larva of 55 h shows a rounded three-layered periostracum. At about 60 h a first intercrystalline organic matrix becomes visible beneath the 60 μm wide periostracum which then starts to vault up. At the same time in the center of the shell a new cell type appears from the now evaginating SFI which corresponds to the calcifying outer mantle epithelium of adults.[21, 22] After 72 h the embryonic shell is oval and about 150 × 180 μm in diameter, after 120 h the embryonic shell has 1½ turns and the outer appearance of an adult shell.

Bielefeld and Becker had a first indication for a crystalline inorganic shell from polarizing microscopy (birefringence) and scanning electron microscopy after 45 h growth at 28 °C (slightly faster development than at 25 °C), but no information on its crystallinity or modification was obtained.[21] Therefore we studied newly laid spawning packs of different ages with high-resolution powder diffraction (Figure 1). The samples of 60 and 72 h age were completely X-ray amorphous, whereas in 120 h old eggs first peaks of aragonite appeared. No other crystalline phases were detectable. The pattern of the shell of fully outgrown snails is also shown for comparison in Figure 1. This could indicate that the calcium-containing shell found in ref.[21] after 45 h consists of amorphous calcium carbonate (ACC).

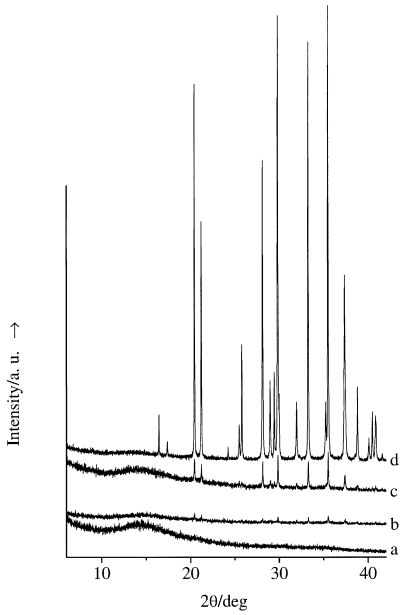

Figure 1. Diffraction pattern of a) 72 hour old eggs, b) 120 hour old eggs, c) 140 hours old eggs, and d) shell of adult snails. 60 hour old eggs were completely amorphous (not shown).

However, there remains a contradiction between the observation of birefringence during early shell formation[21] (that would require an ordered material) by Bielefeld and Becker, and the absence of crystallinity as found in our experiments. This could be due to two reasons. First, the birefringence could result from an organized organic matrix that precedes mineral deposition. Second, the amount of crystalline calcium carbonate (that may even be present in a disordered form leading to broad diffraction peaks) could be too small to be detectable by diffraction, even at a synchrotron source.

The ash content of 72 h old eggs after heating to 1200 °C was 1.6 wt % (thermogravimetry under oxygen). Under the assumption that it consisted of CaO only (from decarboxylation of $CaCO_3$), a maximum content of 2.8 wt % calcium carbonate can be computed. We estimate the detection limit to about 0.2 wt % of crystalline $CaCO_3$ in the current setup. Taking this into account, the observed birefringence must be due either to an ordered organic matrix or to poorly crystalline (but still ordered) calcium carbonate.

As diffraction is sensitive only to crystalline phases, the question remains whether the crystallization starts from amorphous solid precursors, like amorphous calcium carbonate that was proposed as intermediate in biological crystallization processes.[1] In some cases, it was directly detected in organisms, for example in plant cystoliths,[23] in calcareous sponges,[24] and in developing spicules of sear urchin larvae.[25] Recently, calcite phases with high magnesium content were

Abstract in German: *Die Mineralphase (Calciumcarbonat) der Schale der tropischen Süßwasserschnecke Biomphalaria glabrata wurde mit hochauflösender Synchrotron-Röntgenpulverdiffraktometrie und Röntgenabsorptionsspektroskopie (EXAFS) untersucht. Dabei wurden verschiedene Bereiche der Schale vermessen, wobei auch Alters- und Haltungsbedingungen variiert wurden. Die Untersuchung von Gelegen mit 60, 72, 120 und 140 Stunden Alter ergab, dass die ersten Spuren kristallinen Aragonits nach 120 Stunden auftreten. Aus den röntgenabsorptionsspektroskopischen Ergebnissen lässt sich schliessen, dass die aragonitische Struktur bereits in den röntgenamorphen Proben (72 h) vorgebildet ist. In ausgewachsenen Tieren besteht die Schale in allen Fällen aus Aragonit, wobei auch Spuren von Vaterit enthalten sind (< 1.5 %). Im ältesten Teil der Schale (Zentrum) ist der Vaterit-Gehalt am niedrigsten. Er steigt dann in Richtung des Schalenrandes (Mineralisierungszone) an. In noch nicht vollständig ausgewachsenen Schnecken konnte kein Vaterit gefunden werden.*

0947-6539/00/0620-3680 $ 17.50+.50/0 *Chem. Eur. J.* **2000**, *6*, No. 20

prepared by crystallization from stabilized amorphous calcium carbonate phases in vitro.[26]

Infrared[27] and Raman[26] spectroscopy have proved to be valuable methods to distinguish different phases of calcium carbonate. Therefore we have performed IR spectroscopy on the egg samples of different age and compared the results with the fully mineralized shell of an adult snail (Figure 2). Unfortunately, while the spectrum of the mineralized shell perfectly corresponds to aragonite,[27] there are no differences between the three egg samples. In fact, the spectra are all identical to those reported for the soluble organic matrix in the developed shell.[14, 16] We ascribe this result to the small amount of mineral in the egg samples (see above), so that the vibration bands of the mineral are completely masked by the organic material. Unfortunately, no statement on the nature of the mineral is possible by vibrational spectroscopy. There is no easy way of separating organic matrix and mineral in the eggs.

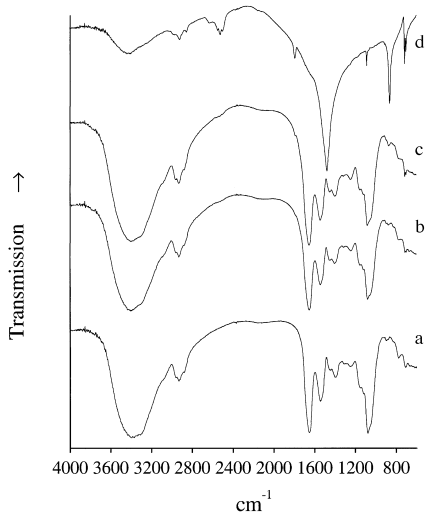

Figure 2. Infrared spectra of a) 72 hours old eggs, b) 120 hours old eggs, c) 140 hours old eggs, and d) shell of adult snails (aragonite). The small content of crystalline material in the eggs is fully masked by the presence of organic matrix, therefore no significant differences are visible between the egg samples.

As another supplementary analytic tool, X-ray absorption spectroscopy (EXAFS) has emerged as versatile tool for analysis of non-crystalline solids.[28, 29] With this method, the local environment around selected elements can be probed on a sub-nanometer scale, as demonstrated in biomineralization for amorphous cystoliths consisting of $CaCO_3$.[23] Information on coordination shells around selected elements (e.g., calcium in this case) is available (interatomic distance, coordination number, mean-square displacement = Debye–Waller factor).

We have carried out Ca K-edge EXAFS spectroscopy on eggs of *Biomphalaria glabrata* of 72, 120, and 140 h age. The results are shown in Figures 3 and 4, together with the simulated data for crystalline aragonite. The numerical results can be found in Table 1.

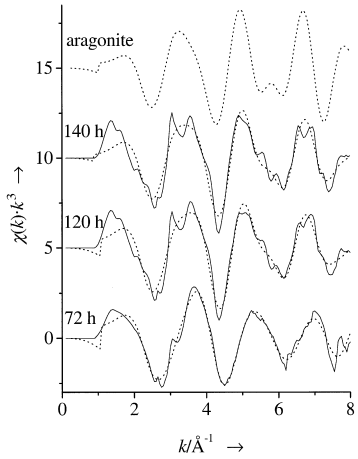

Figure 3. Ca K-edge EXAFS function $\chi(k)$: a) 72 hour old eggs, b) 120 hour old eggs, c) 140 hour old eggs, and d) crystalline aragonite. Solid lines: Experimental data; dotted lines: calculated data.

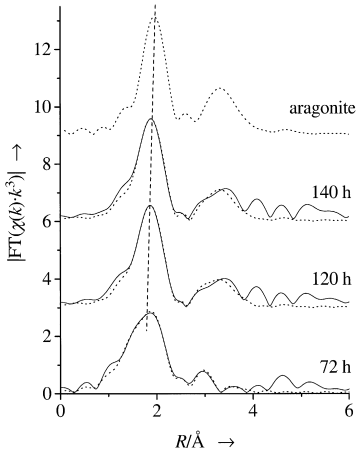

Figure 4. Fourier-transform magnitudes of Ca K-edge EXAFS spectra, giving the radial distribution function around calcium: a) 72 hour old eggs, b) 120 hour old eggs, c) 140 hour old eggs, and d) crystalline aragonite. Solid lines: Experimental data; dotted lines: calculated data; dashed line: increase of the maximum of the first CaO shell from **a** to **d**.

The results indicate that the calcium species present in eggs is already very similar to aragonite, even in the X-ray amorphous sample. However, there is a small shift of the

Table 1. Results of EXAFS fits of eggs during embryonal development.[a]

Sample	Edge jump $\Delta\mu d$	Fit range k/Å^{-1}	Fit range R/Å	E_0/eV	1st shell: 9 O in 2.42–2.65 Å		2nd shell: 3 C in 2.90 Å		3rd shell: 3 C in 3.24–3.41 Å		4th shell: 6 Ca in 3.89–4.11 Å	
					R/Å	$\sigma^2 \times 10^3$/Å^2	R/Å	$\sigma^2 \times 10^3$/Å^2	R/Å	$\sigma^2 \times 10^3$/Å^2	R/Å	$\sigma^2 \times 10^3$/Å^2
eggs, 72 h	≈0.1	1.5–8.7	1.1–4.4	4.39	2.44	30.9	–	–	–	–	3.92	47.0
eggs, 120 h	≈0.4	1.5–9.0	1.1–4.4	4.37	2.47	17.4	2.84	13.4	3.10	35.0	3.95	22.0
eggs, 140 h	≈0.5	1.5–9.0	1.1–4.4	3.79	2.49	17.6	2.88	11.2	3.21	46.9	3.95	20.2

[a] The 2nd and the 3rd shell of the eggs of 72 h age could not be fitted due to moderate data quality (small edge jump due to small Ca content).

  0947-6539/00/0620-3681 $ 17.50+.50/0

distance R of the first coordination shell around calcium to lower values with decreasing age of the eggs: 2.49/2.47/2.44 Å (Figure 5). This points to a change in the solid phase during embryogenesis, possibly going into the direction of crystalline aragonite.

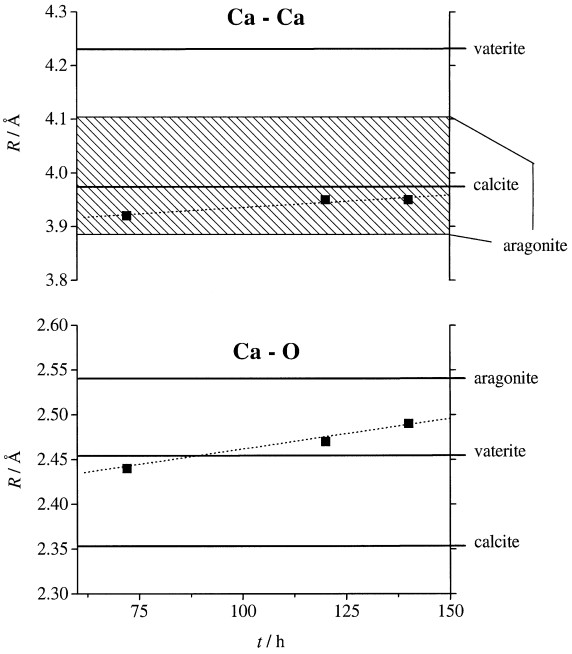

Figure 5. Interatomic distances of the first shell (Ca–O; bottom) and the fourth shell (Ca-6–Ca; top) from Ca K-edge EXAFS. The crystallographic distances of the three polymorphic phases are denoted as lines (weighted averages given for Ca–O).

The values for the first oxygen coordination shells are 2.36 Å (6 O) for calcite, 2.30 Å (1 O)/2.45 Å (2 O)/2.54 Å (2 O) for vaterite, and 2.42 Å (1 O)/2.44 Å (2 O)/2.52 Å (2 O)/2.55 Å (2 O)/2.65 Å (2 O) for aragonite.[23] The weighted average values for the first shell are 2.36 Å (6 O; calcite), 2.46 Å (5 O; vaterite) and 2.53 Å (9 O; aragonite). Calcite as well as vaterite have significantly smaller Ca–O distances for the first shell than aragonite. The first oxygen coordination shell around calcium was refined to 2.35 Å in calcite and 2.36 Å in calcite-like amorphous calcium carbonate in plant cystoliths,[23] therefore we can conclude that the initial calcium carbonate phase in *Biomphalaria glabrata* is not of calcitic nature.

A distinction between aragonite and vaterite is possible by comparing the distances for the first shell of calcium neighbors. The crystallographic values are 3.98 Å for calcite, 3.89 – 4.11 Å for aragonite, and 4.24 Å for vaterite (coordination number 6 in all cases). As the refinement of this shell was possible with a distance of 3.95 Å for eggs of 120 and 140 h, we can conclude that vaterite is not present in major amounts. The characteristic distances for the three polymorphs are depicted in Figure 5.

Summarizing these observations, we may conclude that the structure of aragonite is already preformed in the completely (72 h) and mostly (120 h) amorphous embryonic shells: We have the short-range order of aragonite, but no long-range order as the shell is X-ray amorphous. The degree of order is small in the youngest embryonic shells as revealed by the almost complete absence of shells beyond the first Ca–O shell. There are no indications that vaterite or calcite are formed initially, as it could have been expected for vaterite according to Ostwald's step rule.

To make this interpretation quite clear it must be noted that the EXAFS results for the developing shells point to aragonite and seem to exclude calcite and vaterite. Given the nature of EXAFS as a short-range method, this proof is not as strict as it would be if we had a crystalline phase and an unequivocal diffractogram of it. Additionally, a mixture of amorphous calcium carbonate with small amounts of crystalline (or crystallizing) aragonite cannot be excluded by EXAFS (but higher contents of crystalline aragonite can be excluded due to the diffraction data).

Aragonite is the main inorganic constituent in the shell of fully developed *Biomphalaria glabrata*. The amount of the organic matrix is very small (ca. 0.9 wt %) compared with the inorganic part of the shell. In order to check the phase purity of the shell, high-resolution diffraction experiments were carried out on different parts of the shell, following the observation by Günther and Wolf that small amounts of vaterite can be present in the shell of *Biomphalaria glabrata* (C. Günther and G. Wolf, Freiberg, unpublished results). The shell of animals of different age and keeping conditions was studied here.

In order to detect a spatial variation of the vaterite content, the shell of each animal was divided into four parts as depicted in Figure 6. Each experiment was carried out with the combined shell fractions of about 20 animals, thereby

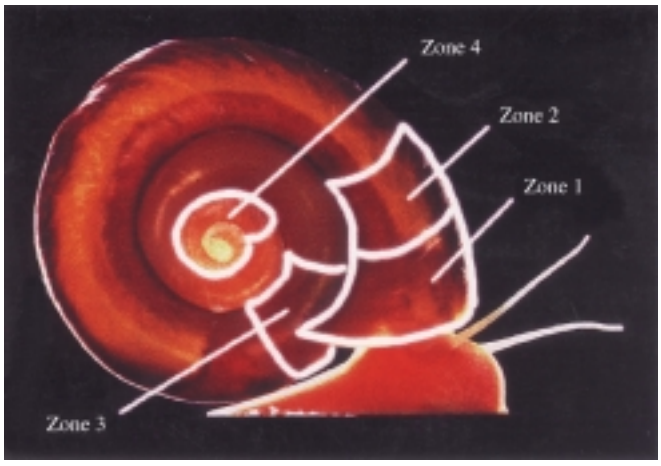

Figure 6. The shell of *Biomphalaria glabrata* with different locations from which samples were investigated.

variations from animal to animal were minimized. The shell consisted of well-crystallized aragonite in all cases, but indeed, small amounts of vaterite were detectable in most samples. It must be emphasized that the quantification of the very small amounts of vaterite besides the highly crystalline aragonite as given in Table 2 was only possibly through the use of synchrotron X-ray diffraction. With conventional X-ray sources, the relative error is higher by at least one order of

0947-6539/00/0620-3682 $ 17.50+.50/0 *Chem. Eur. J.* **2000**, *6*, No. 20

Table 2. Vaterite content in the shell of *Biomphalaria glabrata* as determined by Rietveld refinement.[a]

Sample	Zone of shell (see Figure 6)	Aragonite [%]	Vaterite [%]
eggs, 60 h	–	completely amorphous	
eggs, 72 h	–	completely amorphous	
eggs, 120 h	–	traces of aragonite	
eggs, 140 h	–	some aragonite	
adult snail	1	99.82, 99.42	0.18, 0.58
adult snail	2	99.35, 99.24	0.65, 0.76
adult snail	3	99.79, 98.92	0.21, 1.08
adult snail	4	99.91, 99.95	0.09, 0.05
juvenile snail	1	100.00	0.00
juvenile snail	2	100.00	0.00
juvenile snail	3	99.96	0.04
juvenile snail	4	99.96	0.04
adult, starvation for 3 weeks	1	98.66	1.34
adult, starvation for 3 weeks	2	99.31	0.69
adult, starvation for 3 weeks	3	99.37	0.63
adult, starvation for 3 weeks	4	99.93	0.07
adult, starvation for 1 week	1	99.78	0.22

[a] Two sets of adult animals were studied.

magnitude. A Rietveld refinement plot on a sample with a high content of vaterite (1.34%) is displayed in Figure 7. All results are collected in Table 2.

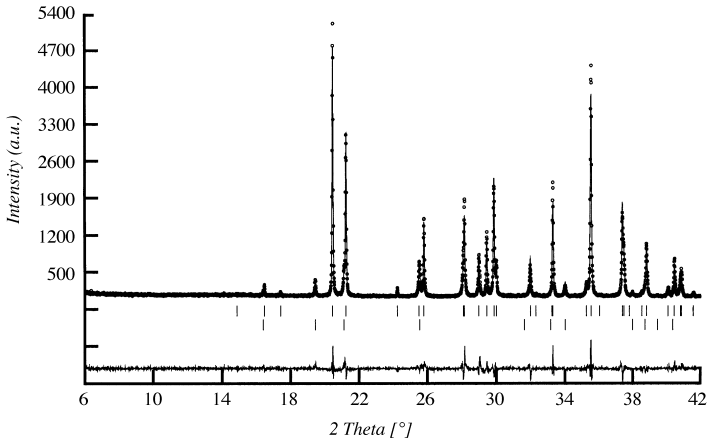

Figure 7. Rietveld refinement of diffraction pattern of the shell of *Biomphalaria glabrata*. On the top, the diffraction pattern is shown. Open circles correspond to experimental points, the solid line to the calculated curve. The marks below the pattern denote the calculated peak positions for aragonite (upper row) and vaterite (lower row). At the bottom, a difference plot (experimental minus calculated data) is shown (1.34% vaterite for this diffractogram).

Snails start growing from the inside, that is upon aging, they add new convolutions (turns) to their shell. The oldest part of the shell is the interior (zone 4 in Figure 6), the youngest part is the shell margin (zone 1). The spatial variation of the vaterite content in the shell is shown in Figure 8. Two sets of adult animals with a shell diameter of 17 ± 1 mm and one set of juvenile animals with a shell diameter of 8 ± 1 mm were studied, as well as two sets of adult animals that were kept without food for one and three weeks, respectively. The two latter populations were introduced in order to verify the effect of starvation on shell formation. It is known that mineralization is strongly affected by malnutrition.[30] The following observations can be made from Figure 8 and from Table 2:

1. Juvenile snails do not form a safely detectable amount of vaterite. Note that the zones 1 to 4 for juvenile animals are all close to the center of the shell.
2. The oldest part of the shell, zone 4, contains little or no vaterite.
3. Prolonged starvation (three weeks) appears to increase the vaterite content. However, this conclusion is based on only one data point.

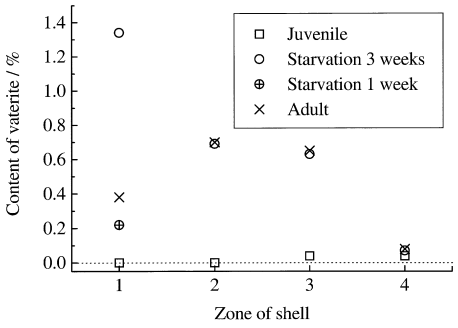

Figure 8. Spatial variation of vaterite content as determined by Rietveld refinement. The values for the adult animals have been averaged from two experiments (see Table 2).

Thus, the vaterite content increases with decreasing age of the shell, that is the smallest amount of vaterite is found in the oldest part of the shell, the center of the snail (zone 4). We may conclude that during mineralization of the shell in adult animals, vaterite is deposited in the newly formed shell, either to perform a specific function or as the result of a disturbed mineralization process. Another explanation could be the formation of vaterite during repair of mechanically damaged parts of the shell, as found by Wilbur and Watabe (see below). This would probably lead to an accumulation of vaterite on the exterior of the shell (below the periostracum, the external organic layer on the shell). Unfortunately, the very high mechanical strength of the shell (Vickers hardness of about 370) together with its brittleness, have so far prevented the study of the vaterite concentration as a function of depth in the shell.

A number of authors has also found vaterite in mollusk shells. Wilbur and Watabe studied the content of the different polymorphic phases after inducing defects in shells of different mollusks that usually formed only one polymorph (calcite or aragonite). They found that the snail *Viviparus intertextus* formed all three different polymorphs simultaneously. During regeneration of the defect (hole in the shell) for 30 days, vaterite was formed first and then replaced mostly by aragonite, while the calcite content remained mostly constant. An increase in the keeping temperature led to a decrease of the vaterite content in favor of aragonite.[31] Vaterite was found as early as 1931 in the shell of this organism, being postulated as a precursor of aragonite.[32–34] If the formation of vaterite occurs in a controlled way by the organism, a detailed analysis of the biological macromolecules that are present in the mineralized shell as a function of vaterite content would help explaining the mechanism of this mineralization process.

It has been found by several authors that these macromolecules (e.g., peptides) exert a strong control over the polymorphic phase formed.[24, 35, 36] However, nothing is known so far about the mechanism of the vaterite–aragonite transition (suggestions include a dissolution–reprecipitation process or a solid state phase transformation).[1]

Conclusion

The mineral phase of the shell of *Biomphalaria glabrata* is formed between about 60 and 120 h in eggs. The first stage is an amorphous calcium carbonate phase in which the structure of aragonite is already preformed. There are no indications for other crystalline calcium carbonate phases (calcite or vaterite). Upon aging of the animal, the shell contains small amounts of vaterite (up to ca. 1.4%). The reason for the occurence of this unexpected phase is unknown. It may either have a specific function in the shell (such as forming a composite with aragonite or acting as calcium storage) or it may simply be an indication for a disturbed mineralization process. As there are no indications by any method that vaterite is present in embryonic snails, we can rule out a consecutive shell formation in which metastable vaterite is formed first and later transformed into the thermodynamically more stable aragonite. Consequently, two different mechanisms must be involved in embryonic shell formation (aragonite from amorphous $CaCO_3$; but note that aragonite formation de novo cannot be ruled out) and shell formation or repair in adult snails (aragonite with some vaterite).

Experimental Section

Animals: The snails of the species *Biomphalaria glabrata* (Say) were kept in running tap water at 25 °C in a 12-to-12 hour light and dark cycle. Standard snails were fed ad libitum with a modified diet consisting of lettuce, milk powder, wheat germs, and alginate.[37] Parts of the shells from 20 snails per group were broken with a forceps and ground. The samples were kept at room temperature at all times. Starving animals were cleaned daily to prevent coprophagy. Newly-laid spawning packs were separated, collected at defined time intervals, lyophylized to remove the water content, and ground. Shell edges from standard and starving snails were examined by scanning electron microscopy to check the nutritional condition.

Extended X-ray absorption fine structure (EXAFS): The experiments were carried out at the Hamburger Synchrotronstrahlungslabor (HASYLAB) at Deutsches Elektronen-Synchrotron (DESY), Hamburg, at beamline E4. The DORIS III storage ring was operated at 4.5 GeV positron energy and currents of 70–150 mA. The incoming synchrotron beam was monochromatized by a Si double-crystal. Experiments were performed at the Ca K-edge (ca. 4038 eV) in transmission mode at room temperature. The ground samples were fixed in a thin layer on adhesive tape. For quantitative data evaluation we used the programs AUTOBK and FEFFIT of the University of Washington package.[38] Theoretical standards were computed with the program FEFF 6.01a[39] using the crystal structure of aragonite by de Villiers as input data.[40] All fits were carried out with k^3-weighted data in R-space. The amplitude reduction factor S_0^2 was fixed to 0.60. The coordination numbers for all fitted shells were kept to the values derived from the aragonite crystal structure (9 O, 3 C, 3 C, 6 Ca). The restriction introduced into the fits by keeping the coordination numbers constant does not significantly influence the shell distances obtained from the fit. This is typical for EXAFS evaluations as shell radius (corresponding to wavelength of EXAFS oscillation) and coordination number (corresponding to amplitude of EXAFS oscillation) are not strongly correlated. Fits with other coordination numbers (6, 12) gave the same shell distances within the usual error margin of EXAFS experiments (±0.02 Å), therefore the differences in shell radius discussed for the different $CaCO_3$ polymorphs are significant. The EXAFS spectrum of aragonite was simulated using FEFF 6.01a (four shells with N and R from crystallography; $\sigma^2 = 10 \times 10^{-3}$ Å^2).

High resolution X-ray powder diffractometry: Data were recorded at HASYLAB at beamline B2 under the same storage ring conditions as described above. The incoming synchrotron beam was monochromatized with a Ge(111) double-crystal to wavelengths of 1.1987 Å, 1.2076 Å, and 1.2066 Å, respectively. The ground samples were fixed on capton foils with acetone and studied in transmission mode using a secondary Ge(111) analyzing crystal. For profile fitting and Rietveld refinement we used the program FULLPROF,[41] and for quantitative phase analysis the method of Hill and Howard.[42] As input data, we used the aragonite structure by de Villiers[40] and the vaterite structure by Kamhi.[43] The error associated with the determination of the vaterite content in these experiments is estimated to ±0.2%. That means that vaterite concentrations below 0.2% cannot be safely detected. The main reasons for this uncertainty are counting statistics (but note that this error is considerably smaller in the synchrotron-based experiment than with conventional X-ray tubes due to higher beam intensity and far better signal-to-noise ratio) and the intrinsic correlation between the means-square displacement factor (Debye–Waller factor) and the scale factor for each phase in the Rietveld plot.

Acknowledgements

We thank Markus Tischer (Hamburg) for experimental assistance, and we are grateful to HASYLAB at DESY for generous allocation of beamtime. Financial support by the Deutsche Forschungsgemeinschaft (DFG) and the Fonds der Chemischen Industrie (FCI) is also gratefully acknowledged. We thank Steve Weiner (Rehovot) for helpful discussions.

[1] H. A. Lowenstam, S. Weiner, *On biomineralization*, Oxford University Press, **1989**.
[2] L. Addadi, S. Weiner, *Angew. Chem.* **1992**, *104*, 159–176; *Angew. Chem. Int. Ed. Engl.* **1992**, *31*, 153–169.
[3] S. Mann, *J. Mater. Chem.* **1995**, *5*, 935–946.
[4] S. Mann, *Biomimetic Materials Chemistry*, VCH, Weinheim, **1996**.
[5] S. Weiner, L. Addadi, *J. Mater. Chem.* **1997**, *7*, 689–702.
[6] S. Mann, *J. Chem. Soc. Dalton Trans.* **1997**, 3953–3961.
[7] R. Kniep, S. Busch, *Angew. Chem.* **1996**, *108*, 2788–2791; *Angew. Chem. Int. Ed. Engl.* **1996**, *35*, 2624–2626.
[8] G. Falini, S. Fermani, M. Gazzano, A. Ripamonti, *Chem. Eur. J.* **1997**, *3*, 1807–1814.
[9] G. A. Ozin, N. Varaksa, N. Coombs, J. E. Davies, D. D. Perovic, M. Ziliox, *J. Mater. Chem.* **1997**, *7*, 1601–1607.
[10] J. M. Marentette, J. Norwig, E. Stöckelmann, W. H. Meyer, G. Wegner, *Adv. Mater.* **1997**, *9*, 647–651.
[11] K. Schwarz, M. Epple, *Chem. Eur. J.* **1998**, *4*, 1898–1903.
[12] J. Küther, R. Seshadri, W. Tremel, *Angew. Chem.* **1998**, *110*, 3196–3199; *Angew. Chem. Int. Ed.* **1998**, *37*, 3044–3047.
[13] A. Ripamonti, G. Falini, S. Fermani, M. Gazzano, *Chem. Eur. J.* **1998**, *4*, 1048–1052.
[14] J. C. Marxen, W. Becker, *Comp. Biochem. Physiol.* **1997**, *118B*, 23–33.
[15] U. Plate, S. Arnold, T. Kotz, U. Stratmann, H. P. Wiesmann, H. J. Höhling, *Conn. Tissue Res.* **1998**, *38*, 149–157.
[16] J. C. Marxen, M. Hammer, T. Gehrke, W. Becker, *Biol. Bull.* **1998**, *194*, 231–240.
[17] P. Ducy, M. Starbuck, M. Priemel, J. Shen, G. Pinero, V. Geoffroy, M. Amling, G. Karsenty, *Genes Dev.* **1999**, *13*, 1025–1036.
[18] U. Bielefeld, K. Zierold, K. H. Körtje, W. Becker, *Histochem. J.* **1992**, *24*, 927–938.
[19] U. Bielefeld, K. H. Körtje, H. Rahmann, W. Becker, *J. Moll. Stud.* **1993**, *59*, 323–338.
[20] U. Bielefeld, W. Peters, W. Becker, *Acta Zool.* **1993**, *74*, 181–193.
[21] U. Bielefeld, W. Becker, *Int. J. Dev. Biol.* **1991**, *35*, 121–131.
[22] U. Bielefeld, K. H. Körtje, W. Becker, *Zool. Anz.* **1992**, *228*, 45–59.

  0947-6539/00/0620-3684 $ 17.50+.50/0

[23] M. G. Taylor, K. Simkiss, G. N. Greaves, M. Okazaki, S. Mann, *Proc. R. Soc. Lond. B* **1993**, *252*, 75–80.
[24] J. Aizenberg, G. Lambert, L. Addadi, S. Weiner, *Adv. Mater.* **1996**, *8*, 222–226.
[25] E. Beniash, J. Aizenberg, L. Addadi, S. Weiner, *Proc. R. Soc. London B* **1997**, *264*, 461–465.
[26] S. Raz, S. Weiner, L. Addadi, *Adv. Mater.* **2000**, *12*, 38–42.
[27] F. A. Andersen, L. Brecevic, *Acta Chem. Scand.* **1991**, *45*, 1018–1024.
[28] G. N. Greaves, W. Smith, E. Giulotto, E. Pantos, *J. Non-cryst. Solids* **1997**, *222*, 13–24.
[29] H. Bertagnolli, T. S. Ertel, *Angew. Chem.* **1994**, *106*, 15–37; *Angew. Chem. Int. Ed. Engl.* **1994**, *33*, 45–66.
[30] J. Marxen, unpublished results.
[31] K. M. Wilbur, N. Watabe, *Ann. N.Y. Acad. Sci.* **1963**, 82–112.
[32] F. K. Mayer, *Jena. Z. Naturwiss.* **1931**, *65*, 487–512.
[33] K. G. v. Levetzow, *Jena. Z. Naturwiss.* **1932**, *66*, 41–108.
[34] E. Kessel, *Z. Morphol. Oekol. Tiere* **1933**, *27*, 9–198.
[35] G. Falini, S. Albeck, S. Weiner, L. Addadi, *Science* **1996**, *271*, 67–69.
[36] C. M. Zaremba, A. M. Belcher, M. Fritz, Y. Li, S. Mann, P. K. Hansma, D. E. Morse, J. S. Speck, G. D. Stucky, *Chem. Mater.* **1996**, *8*, 679–690.
[37] W. Becker, I. Lamprecht, *Z. Parasitenk.* **1977**, *53*, 297–305.
[38] E. A. Stern, M. Newville, B. Ravel, Y. Yacoby, D. Haskel, *Physica B* **1995**, *208–209*, 117–120.
[39] S. I. Zabinsky, J. J. Rehr, A. Ankudinov, R. C. Albers, M. J. Eller, *Phys. Rev. B* **1995**, *52*, 2995.
[40] J. P. R. de Villiers, *Am. Mineral.* **1971**, *56*, 758–772.
[41] J. Rodriguez-Carvajal, *Abstracts of the Satellite Meeting on Powder Diffraction of the XV Congress of the IUCr*, *Toulouse*, *France*, **1990**, p. 127.
[42] R. J. Hill, C. J. Howard, *J. Appl. Crystallogr.* **1987**, *20*, 467–474.
[43] S. R. Kamhi, *Acta Crystallogr.* **1963**, *16*, 770–772.

Received: January 21, 2000 [F2252]